

Effective Rheology of Immiscible Two-Phase Flow in Porous Media

Santanu Sinha* and Alex Hansen†

Department of Physics, Norwegian University of Science and Technology, N-7491 Trondheim, Norway

(Dated: May 7, 2018)

We demonstrate through numerical simulations and a mean-field calculation that immiscible two-phase flow in a porous medium behaves effectively as a Bingham viscoplastic fluid. This leads to a generalized Darcy equation where the volumetric flow rate depends quadratically on an excess pressure difference in the range of flow rates where the capillary forces compete with the viscous forces. At higher rates, the flow is Newtonian.

PACS numbers: 47.56.+r, 47.55.Ca, 47.55.dd, 89.75.Fb

The simultaneous flow of immiscible fluids in porous media [1–3] lies at the heart of a wide range of important applications ranging from oil recovery to ground water management. Within the statistical physics community, there has been considerable interest in this problem since the eighties when the fractal structure of fluid invasion was discovered and explored [4, 5]. Such invasion phenomena are transient and may be characterized by the macroscopic flow parameters, such as injected pore volumes of invading fluids change on the same time scale as those associated with the internal flow. Much less attention, however, has been offered to *steady state flow* which occurs when macroscopic parameters change slowly compared to those associated with the internal flow [6–12].

The steady state has recently been studied experimentally by Tallakstad *et al.* [13, 14] in a two-dimensional Hele-Shaw cell filled with glass beads. There are 15 evenly spaced tubes at one edge of the cell. Air and glycerol are injected at equal rates through each alternate inlet. Fluids leave at the opposing edge, which is kept open. The other two edges of the cell, perpendicular to the direction of overall flow, are closed. As the two immiscible fluids move along the Hele-Shaw cell, they form interpenetrating clusters separated by interfaces. This constitutes the steady state.

The steady state is characterized by a number of macroscopic parameters: Capillary number Ca , viscosity ratio M , total volumetric flow rate Q , non-wetting fractional flow rate F_{nw} , non-wetting saturation S_{nw} and pressure P . The capillary number is the ratio between the typical viscous pressure drop across the pores and the typical capillary force due to the interface between

the fluids. Tallakstad *et al.* observed that the average pressure gradient ΔP throughout the system scales as a power law with the capillary number Ca as,

$$\Delta P \sim Ca^\beta, \quad (1)$$

where $\beta = 0.54 \pm 0.08$.

More recently, Rassi *et al.* [15] have measured the exponent β which varies in the range of 0.3 to 0.45 depending on the saturation, in steady-state two-phase flow of water and air in a three-dimensional porous medium constructed from glass beads.

These observations have profound implications on the description of multiphase flow in porous media. An important application would be in the reservoir simulators, used in the exploitation of oil reservoirs. They are based on effective transport equations for the fluids where a linear relation between the pressure gradients and flow rates [1] is assumed so far.

We will in this Letter demonstrate that, in the regime where capillary forces are comparable to the viscous forces (low Ca), the capillary effects at the interfaces between the immiscible fluids effectively creates a yield threshold, making the fluids reminiscent of a Bingham viscoplastic fluid [16, 17] in the porous medium — i.e. a fluid possessing a yield stress and a constant effective viscosity. This introduces a overall threshold pressure ΔP_c in the system due to the random distribution of capillary pressure thresholds. We therefore propose, and will show in the following via numerical simulations and a mean field calculation, that the steady-state two-phase flow in porous media in this flow regime is governed by a generalized Darcy equation

$$Q = -C \frac{A}{L} \frac{K(S_{nw})}{\mu_{\text{eff}}(S_{nw})} \text{sgn}(\Delta P) \begin{cases} (|\Delta P| - \Delta P_c(S_{nw}))^2 & \text{if } |\Delta P| > \Delta P_c, \\ 0 & \text{if } |\Delta P| \leq \Delta P_c, \end{cases} \quad (2)$$

where sgn is the sign function. Here A is the cross section of the representative elementary volume, L is its length, C a constant with units of inverse pressure, $K(S_{nw})$ the

effective permeability which depends on the saturation S_{nw} and $\mu_{\text{eff}}(S_{nw})$ is the saturation-weighted viscosity given by $S_{nw}\mu_{nw} + (1 - S_{nw})\mu_w$, where μ_w and μ_{nw} are

the viscosities of wetting and non-wetting fluids respectively.

As a result, the correct scaling relation in general between ΔP and Ca is not Eq. (1), but

$$(|\Delta P| - \Delta P_c) \sim \text{Ca}^\beta, \quad (3)$$

with $\beta = 1/2$ for low Ca . The relation (1) is just a special case of this relation where $\Delta P_c \approx 0$.

There is another flow regime for high Ca where the flow is linear with the excess pressure drop which corresponds to $\beta = 1$. This regime is therefore characterized by the standard Darcy equation $Q = -(A/L)(K/\mu_{\text{eff}}(S_{nw}))\Delta P$. Here $|\Delta P| \gg \Delta P_c$ and the threshold pressure is not relevant.

The physical existence of the global threshold pressure ΔP_c and the quadratic and linear dependence of Q on $(|\Delta P| - \Delta P_c)$ in the two regimes for the system of immiscible fluids can be understood very intuitively following the argument of Roux and Herrmann [17] for networks with link conductances having characteristics like a Bingham fluid: The essential ingredient is a threshold pressure for each link, distributed according to some probability density. The sum over all the thresholds over a continuous flow path throughout the entire system gives the total threshold pressure along that path and ΔP_c corresponds to the minimum sum among all such possible paths. Now, if we raise the pressure difference across the network by a value dP , a number $d\mathcal{N}$ of tubes will cross their flow thresholds. With a reasonably smooth distribution of thresholds, we will have that $d\mathcal{N} \propto dP$. The conductance of the network Σ will then change by an amount $d\Sigma$, and $d\Sigma \propto d\mathcal{N} \propto dP$. An integration over this equation leads to Eq. (2) with the appearance of ΔP_c . Moreover, at a very high value of P , when all the links have crossed their individual flow thresholds, each link behaves linearly with excess pressure drop, making Σ constant with P and effectively the overall flow rate becomes linear with the excess pressure drop in the high Ca regime.

In the following, we will first present our numerical simulations. Afterwards, we will derive the effective Darcy equation (2), adapting the mean-field calculation of the conductivity of heterogeneous conductors by Kirkpatrick [18].

In our numerical studies, the porous medium is modeled by a two-dimensional network of tubes, forming a square lattice tilted by 45° with respect to the imposed pressure gradient. Two immiscible fluids, one is more wetting than the other with respect to the pore walls, flow inside the tubes. Disorder is introduced in the system by choosing the radius r of each tube randomly from a uniform distribution of random numbers in the range $[0.1l, 0.4l]$, where l is the length of the tubes. In order to incorporate the shape of the pores in between spherical particles (beads) that introduces the capillary effect in the system, each tube is considered hour-glass shaped so

that the capillary pressure p_c at a meniscus at position x is proportional to $[2\gamma/r][1 - \cos(2\pi x/l)]$ where γ is the surface tension [2, 19].

The flow is driven by setting up an external global pressure drop. The local flow rate q in a tube with a pressure difference Δp between the two ends of that tube follows the Washburn equation of capillary flow [2, 19]

$$q = -\frac{ak}{\mu_{\text{eff}}(s_{nw})l} \left(\Delta p - \sum p_c \right) = -\sigma_0 (\Delta p - \Sigma p_c), \quad (4)$$

where $k = r^2/8$ is the permeability for cylindrical tubes. The conical shape of the tubes leads only to an overall geometrical factor. Here a is the cross-sectional area of the tube and $\mu_{\text{eff}}(s_{nw})$ is the volume average of the viscosities of the two phases present inside the tube. Hence, it is a function of the saturation s_{nw} in the tube. The sum over p_c runs over all menisci within the tube. σ_0 is thus the tube conductivity. The set consisting of one equation (4) per tube, together with the Kirchhoff equations balancing the in and out flow at each node are then solved using Cholesky factorization combined with a conjugate gradient solver. The system is then integrated in time using an explicit Euler scheme. Inside a tube all menisci move with a speed determined by q . When a meniscus reaches the end of a tube, new menisci are formed in the neighboring tubes. Further details of the model and how the menisci are moved can be found in [9, 19].

The steady-state condition in the simulation is achieved in two ways. The conventional way is to use bi-periodic boundary conditions (BP), by connecting the inlet and outlet rows so that the network takes a toroidal topology [10]. It is then initialized by filling with two fluids randomly or sequentially so that the network attains the desired saturation S_{nw} . As the system is closed in this boundary condition, the saturation of the network S_{nw} is an independent parameter which remains constant throughout the simulation along with the total flow rate Q whereas the fractional flow F_{nw} fluctuates over time.

It is not possible to implement bi-periodic boundary condition in the experiments by Tallakstad *et al.* [13, 14], where two fluids are injected at one edge of the system through a series of alternate inlets and the opposite edge is kept open. Flow rates of the two fluids may be controlled independently there. The control parameters in this case are the total flow rate Q and the fractional flow F_{nw} whereas the saturation S_{nw} fluctuates. Therefore, in order to have a close emulation of the experimental system, we also implement open boundary conditions (OB) in our simulation here, controlling the individual flow rates of inlet links. The simulation starts with injecting the two fluids with constant flow rates in a system completely saturated with the wetting fluid. Both drainage and imbibition therefore takes place at the pore level creating new menisci. Away from the inlets, the fluids mix and a steady state is attained as in the experiment.

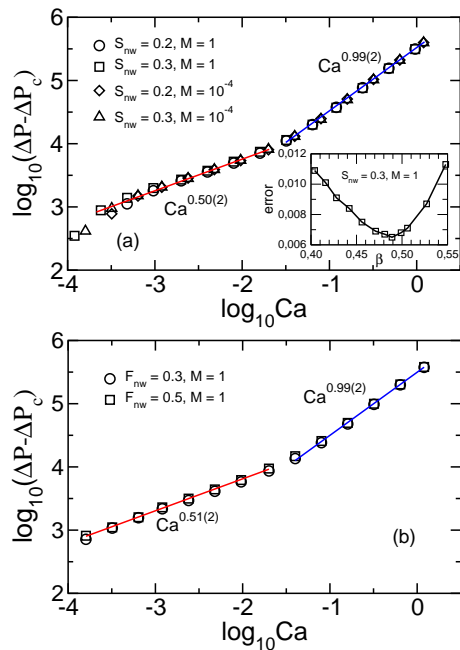


FIG. 1. Scaling of excess steady-state pressure drop ($|\Delta P| - \Delta P_c$) (in Pa) with capillary number Ca for (a) BP and (b) OB boundary conditions. The threshold pressure ΔP_c have determined from minimizing the least square fit errors. This minimization is shown as a function of β in the inset of (a).

Simulations are performed with constant flow rate Q which sets the capillary number Ca given by $Ca = \mu_{\text{eff}} Q / (\gamma A)$. A range of Ca from 10^{-4} to 1 is considered for a network of 64×64 links and an average over 10 different samples is taken for each simulation. We report results for $M = 1$ and 10^{-4} with $S_{nw} = 0.2$ and 0.3 for BP, and $M = 1$ with $F_{nw} = 0.3$ and 0.5 for OB. The steady state is identified from the total pressure drop ΔP , which starts to fluctuate over an average value as steady state is reached. By increasing and then lowering the total flux Q we also verify that it returns to the same steady state. In order to verify Eq. (3), we now need to calculate ΔP_c . Roux and Herrmann [17], for their Bingham system, determined ΔP_c by decreasing the external current from a large value and identifying the current paths by a search algorithm. This procedure is not feasible here as the flow patterns and menisci positions change with global flow rate and time due to fluid instabilities. Moreover, it is also not possible to follow this in experiments as it would necessitate the knowledge of flow rates at every single pore. We therefore measure ΔP_c with a minimization procedure. A series of trial ΔP_c values are considered, for which the slope (β) and the least square fit errors, when fitted to Eq. (3), are calculated. ΔP_c is then identified corresponding to the minimum value of the error or the best fit. This is shown in the inset of Fig. 1(a) for $M = 1$ and $S_{nw} = 0.3$. In Table I, the absolute values of all ΔP_c s, identified by the same procedure,

(a) Biperiodic (BP)

S_{nw}	M	P_c (KPa)
0.2	1	3.45 ± 0.05
0.3	1	5.10 ± 0.05
0.2	10^{-4}	3.45 ± 0.05
0.3	10^{-4}	5.10 ± 0.05

(b) Open (OP)

F_{nw}	M	P_c (KPa)
0.3	1	6.55 ± 0.05
0.5	1	6.15 ± 0.05

TABLE I. Values of threshold pressures (ΔP_c) measured by minimizing the least square fit errors for different parameters and boundary conditions.

are listed. In Fig. 1, ($|\Delta P| - \Delta P_c$) is then plotted with Ca for (a)BP and (b)OB according to Eq. (3). Interestingly, for different saturations (S_{nw}), fractional flows (F_{nw}) and boundary conditions, the minimum error corresponds to different values of ΔP_c but the same value for $\beta = 0.5$ within error bar for low Ca regime. More surprisingly, ΔP_c is found independent to the viscosity ratio which is a strong support towards its intuitive physical description stated before. As ΔP_c is related to the sum of capillary thresholds (p_c) over connecting paths and p_c does not depend on the viscosities, ΔP_c also should not and that is what we found here. A sharp crossover is also seen for high Ca regime with $\beta = 1$ where the flow is linear characterized by standard Darcy equation.

In the experiments by Rassi *et al.* [15], the exponent β , when measured according to Eq. (1) is found to vary from 0.30 to 0.45 depending on the saturation. A preliminary numerical study [20] assuming Eq. (1) using a very similar model with only BP, also reports similar dependency of β on saturation with a visible curvature in the scaling plots. These clearly indicate a non-zero ΔP_c that has been ignored hence resulting in a wandering value of β . Interestingly, the same experimental data by Rassi *et al.* [15] are found consistent with $\beta = 1/2$ when reanalyzed using Eq. (3) [22]. In the experiment by Tallakstad *et al.* [13, 14], β is found as 0.54 ± 0.08 with scaling relation (1) which is due to the fact that one of the fluids was percolating in their system [21], making $\Delta P_c = 0$.

In support of our numerical results, we now derive the generalized Darcy equation, Eq. (2) in a mean field approximation. Eq. (4) describes instantaneous the flow in a single tube. Time averaging this equation under steady state conditions leads to an effective flow equation for the single tube [23]

$$q = -\sigma_0 \text{sgn}(\Delta p) \begin{cases} \sqrt{\Delta p^2 - \Delta p_c^2} & \text{if } |\Delta p| > \Delta p_c, \\ 0 & \text{if } |\Delta p| \leq \Delta p_c. \end{cases} \quad (5)$$

where Δp_c is an effective flow threshold that depends on the shape of the tube. The effective viscosity that enters into σ_0 is the saturation-weighted sum of the viscosities of each liquid, where the saturation is time averaged over the tube.

The square root singularity near Δp_c is caused by a

saddle-node bifurcation and, hence, is a universal feature of the system [24].

The effective conductivity is thus

$$\sigma(\Delta p) = -\frac{dq}{d(\Delta p)} = \sigma_0 \begin{cases} \frac{|\Delta p|}{\sqrt{\Delta p^2 - \Delta p_c^2}} & \text{if } |\Delta p| > \Delta p_c, \\ 0 & \text{if } |\Delta p| \leq \Delta p_c. \end{cases} \quad (6)$$

In the following, we will derive Eq. (2) based on the mean-field theory originally developed for calculating the conductivity of percolating systems by Kirkpatrick [18]. Our starting point is a regular lattice with coordination number z . Each tube in the lattice has a non-linear conductivity $\sigma(\Delta p)$, Eq. (6). The flow thresholds of the tubes are drawn from a spatially uncorrelated probability distribution $\pi(\Delta p_c)$.

The mean-field calculation proceeds by focusing on one tube inside the network. We then replace the rest of the network by an *equivalent homogeneous network* where all tubes have the same conductivity $m(\Delta p)$ so that the tube we have singled out experiences the same average effect from the homogeneous network as from the original

network. We then average over this last conductance and determine $m(\Delta p)$ in a self-consistent way.

There is one caveat. In Kirkpatrick's original calculation, the conductances were assumed to be linear, whereas in our case, the conductances are highly non-linear, see Eq. (6). However, the end result of the calculation,

$$\left\langle \frac{m(\Delta p) - \sigma(\Delta p)}{\left(\frac{z-2}{2}\right) m(\Delta p) + \sigma(\Delta p)} \right\rangle = 0, \quad (7)$$

is the same. This equation provides a self-consistent expression for the equivalent conductivity $m(\Delta p)$.

In terms of the distribution of flow thresholds $\pi(\Delta p_c)$, Eq. (7) becomes

$$\int_0^\infty dp \pi(p) \frac{m(\Delta p) - \sigma(\Delta p)}{\left(\frac{z-2}{2}\right) m(\Delta p) + \sigma(\Delta p)} = 0. \quad (8)$$

We now combine this expression with Eq. (6), finding

$$\int_0^{\Delta p} dp \pi(p) \frac{m(\Delta p) \sqrt{\Delta p^2 - p^2} - \sigma_0 |\Delta p|}{\left(\frac{z-2}{2}\right) m(\Delta p) \sqrt{\Delta p^2 - p^2} + \sigma_0 |\Delta p|} + 1 - \Pi(\Delta p) = 0, \quad (9)$$

where $\Pi(p) = \int_0^p dp' \pi(p')$ is cumulative probability to find a flow threshold less than or equal to p .

By setting $m(\Delta p) = 0$ in Eq. (9), we determine the effective flow threshold $\Delta \bar{p}_c$ for the effective tubes:

$$\Pi(\Delta \bar{p}_c) = \frac{1}{2}. \quad (10)$$

If we now set $\Delta p > \Delta \bar{p}_c$ in Eq. (9) and expand to

lowest order in $m(\Delta p)$, we find

$$m(\Delta p) = \frac{4\sigma_0}{8-z} \pi(\Delta \bar{p}_c) \frac{(\Delta p - \Delta \bar{p}_c)}{\int_0^{\Delta \bar{p}_c} dp \pi(p) \sqrt{1 - \left(\frac{p}{\Delta \bar{p}_c}\right)^2}}, \quad (11)$$

where we have used that $\Pi(\Delta p) - 1/2 = \pi(\Delta \bar{p}_c)(\Delta p - \Delta \bar{p}_c)$ to lowest order. We integrate Eq. (11) and find

$$\bar{q} = -\frac{2\sigma_0}{8-z} \frac{\pi(\Delta \bar{p}_c) \operatorname{sgn}(\Delta p)}{\int_0^{\Delta \bar{p}_c} dp \pi(p) \sqrt{1 - \left(\frac{p}{\Delta \bar{p}_c}\right)^2}} \begin{cases} (|\Delta p| - \Delta \bar{p}_c)^2 & \text{if } |\Delta p| > \Delta \bar{p}_c, \\ 0 & \text{if } |\Delta p| \leq \Delta \bar{p}_c. \end{cases} \quad (12)$$

If there are N tubes in a cross section of the homogeneous network orthogonal to the flow direction, then $Q = N\bar{q}$, $\Delta P = (L/l)\Delta p$ and $\Delta P_c = (L/l)\Delta \bar{p}_c$. Hence, the generalized Darcy equation (2) follows.

There are corrections associated with larger exponents to Eq. (11) originating from two sources. The first one comes from solving Eq. (9). The prefactor of the leading correction from this source is about 7% of the prefactor of the dominating term. The second source of correction terms comes from the linearization of $\Pi(\Delta p) - 1/2$ around

the value $\Delta \bar{p}_c$. There are no reasons to assume strong non-linear corrections in this region.

To summarize, we have demonstrated numerically and through a mean field calculation that steady-state immiscible two-phase flow in a porous medium behaves similar to a Bingham viscoplastic fluid. This leads to a non-linear Darcy equation where the volumetric flow rate depends *quadratically* on an excess pressure drop at capillary numbers at which the capillary forces compete with the viscous forces. At higher flow rates, the flow becomes

Newtonian.

We thank D. Bedeaux, E. G. Flekkøy, S. Kjelstrup, K. J. Måløy and L. Talon for useful discussions. This work was partially supported by the Norwegian Research Council through grant no. 193298. We thank NOTUR for allocation of computer time.

* Santanu.Sinha@ntnu.no

† Alex.Hansen@ntnu.no

- [1] J. Bear, *Dynamics of Fluids in Porous Media* (Dover, New York, 1988).
- [2] F. A. L. Dullien, *Porous Media: Fluid, Transport and Pore Structure, Second Edition* (Academic Press, San Diego, 1992).
- [3] M. Sahimi, *Flow and Transport in Porous Media and Fractured Rock* (VCH, Weinheim, 1995).
- [4] R. Lenormand, E. Tourbol and C. Zarcone, *J. Fluid Mech.* **189**, 165 (1988).
- [5] J. Feder, *Fractals* (Plenum, New York, 1988).
- [6] A. K. Gunstensen and D. H. Rothman, *J. Geophys. Res.* **98**, 6431 (1993).
- [7] D. G. Avraam and A. C. Payatakes, *J. Fluid Mech.* **293**, 207 (1995); D. G. Avraam and A. C. Payatakes, *Transp. Por. Media* **20**, 135 (1995).
- [8] D. G. Avraam and A. C. Payatakes, *Ind. Eng. Chem. Res.* **38**, 778 (1999).
- [9] H. A. Knudsen, E. Aker and A. Hansen, *Transp. Por. Media*, **47**, 99 (2002).
- [10] H. A. Knudsen and A. Hansen, *Phys. Rev. E* **65**, 056310 (2002).
- [11] H. A. Knudsen and A. Hansen, *Eur. J. Phys. B*, **49**, 109 (2006).
- [12] T. Ramstad and A. Hansen, *Phys. Rev. E*, **73**, 026306 (2006).
- [13] K. T. Tallakstad, H.A. Knudsen, T. Ramstad, G. Løvoll, K. J. Måløy, R. Toussaint and E. G. Flekkøy, *Phys. Rev. Lett.* **102**, 074502 (2009).
- [14] K. T. Tallakstad, G. Løvoll, H. A. Knudsen, T. Ramstad, E. G. Flekkøy and K. J. Måløy, *Phys. Rev. E*, **80**, 036308 (2009).
- [15] E. M. Rassi, S. L. Codd and J. D. Seymour, *New J. Phys.* **13**, 015007 (2011).
- [16] G. G. Lipscomb and M. M. Denn, *J. Non-Newtonian Fluids*, **14**, 337 (1984).
- [17] S. Roux and H. J. Herrmann, *Europhys. Lett.* **4**, 1227 (1988).
- [18] S. Kirkpatrick, *Rev. mod. Phys.* **45**, 574 (1973).
- [19] E. Aker, K. J. Måløy, A. Hansen and G. G. Batrouni, *Transp. Por. Media*, **32**, 163 (1998); E. Aker, K. J. Måløy and A. Hansen, *Phys. Rev. E* **58**, 2217 (1998).
- [20] M. Grøva and A. Hansen, *J. Phys. Conf. Ser.* **319**, 012009 (2011).
- [21] K. J. Måløy, private communication (2012).
- [22] S. Codd, private communication (2012).
- [23] S. Sinha, A. Hansen, D. Bedeaux and S. Kjelstrup, in preparation (2012).
- [24] S. H. Strogatz, *Non-Linear Dynamics and Chaos* (Perseus Press, Cambridge, 1994).